Journal of Chromatography A, 1381 (2015) 132–139

Contents lists available at ScienceDirect

Journal of Chromatography A

journal homepage: www.elsevier.com/locate/chroma

Lipidomic profiling of plasma and urine from patients with Gaucher disease during enzyme replacement therapy by nanoflow liquid chromatography–tandem mass spectrometry

Seul Kee Byeon [a], Ju Yong Lee [a], Jin-Sung Lee [b,**], Myeong Hee Moon [a,*]

[a] Department of Chemistry, Yonsei University, Seoul 120-749, South Korea
[b] Department of Pediatrics, Yonsei University College of Medicine, Seoul 120-752, South Korea

ARTICLE INFO

Article history:
Received 13 November 2014
Received in revised form
18 December 2014
Accepted 4 January 2015
Available online 10 January 2015

Keywords:
Gaucher disease
Lipid profiling
Monohexosylceramide (MHC)
nLC–ESI–MS/MS
Enzyme replacement therapy

ABSTRACT

Gaucher disease (GD) is a rare genetic disorder that arises from lipid species, especially monohexosylceramide (MHC), accumulating in different organs. GD results from a β-glucocerebrosidase deficiency, causing metabolic or neurologic complications. This study comprehensively profiled lipids from patients and healthy controls to discover active lipid species related to GD. Most studies have evaluated lipids from one type of biological sample, such as plasma, urine, or spinal fluid, which are the main sources of lipids in human bodies. The purpose of this study, however, was to collect and assess both plasma and urine samples from a group of individuals, explore the lipids, and select characteristic species that show significant differences between controls and patients from the two sources. Also, the response of lipids to enzyme replacement therapy (ERT), which is targeted to reduce excessive lipid accumulation within lysosomes, was investigated by obtaining plasma and urine from patients after receiving the therapy. Most lipid species were found in both plasma and urine but their concentrations differed, and some species were found in either plasma or urine only. Out of 125 plasma and 105 urinary lipids that were identified by nLC–ESI–MS/MS, 20 plasma and 10 urinary lipids were selected as characteristic species for having average concentrations that were significantly increased or decreased in patients by greater than 2-fold. Moreover, the concentrations of most lipids that showed greater than 2-fold of difference in patients decreased after ERT indicating that these species were directly or indirectly affected by the therapy.

1. Introduction

Gaucher disease (GD) is a rare genetic disorder that is inherited recessively and caused by the deficiency or absence of an enzyme called β-glucocerebrosidase. β-Glucocerebrosidase degrades glucosylceramide (GluCer), a type of monohexosylceramide (MHC), inside lysosome [1]. GluCer accumulation in lysosomes eventually gives rise to Gaucher cells in the spleen or liver, causing the affected organs to grow abnormally large. GD is differentiated into three types clinically. Type I GD is the least serious as it causes no visible changes in appearance and no neurological complications. Types II and III involve neurodegenerative problems such as dementia, epilepsy, autism, and Parkinson's disease [2,3]. Type II is the most serious form because it involves severe neurodegenerative problems early in life, and patients tend to die before they reach adolescence. Type III develops during adulthood, so it is not as severe as type II. The incidence of GD is reported to be from approximately 1/111,111 to 1/855 in the Ashkenazi Jewish population, with most of these patients having type I GD. Types II and III are often observed in the Middle East and Asia [4]. GD causes multiple physical and neurological problems that may result in premature death or reduced quality of life. Because GD is of a very specific nature, no complete cure has been developed, but enzyme replacement therapy (ERT), which involves routinely administering the deficient enzyme to a patient, is used to lower levels of the excessive substrate and prevent further organ damage [5]. While GD can be readily detected by a genetic test or protein biomarkers, it is related to altered lipid metabolism, resulting in abnormal

* Corresponding author. Tel.: +82 2 2123 5634; fax: +82 2 364 7050.
** Co-Corresponding author.
E-mail addresses: jinsunglee@yuhs.ac (J.-S. Lee), mhmoon@yonsei.ac.kr (M.H. Moon).

http://dx.doi.org/10.1016/j.chroma.2015.01.004
0021-9673/

MHC accumulation, and is also reported to be associated with phosphatidylcholine (PC) and sphingomyelin (SM) increases [6]. Therefore, detailed lipid profiling of patient body fluids can provide a new perspective on how these lipids are related. Moreover, monitoring lipidomic change during drug intervention will be useful.

The roles of lipids range from storing energy to serving a structural role and signal transduction across cell membranes [7,8]. As many metabolic diseases, such as diabetes, obesity, and atherosclerosis, have been reported to be related to lipids [9,10], lipid chemistry has captured increased attention in the medicinal and lipidomics fields. Of the various classes of lipids, phospholipids (PLs) are the main components of biological membranes. PLs vary in terms of the polar head group, length of the acyl chain, and degree of unsaturation. Sphingolipids (SL) such as SM and ceramides (Cer), including MHC and dihexosylceramides (DHC), are the second most abundant lipid class. As lipids are directly or indirectly involved in the development of diseases, studies have been performed to unveil the relationship between lipids and diseases, such as prostate cancer [11,12], breast cancer [13,14], ovarian cancer [15], colorectal cancer [16], and coronary artery disease [17].

Analysis of lipids has rapidly evolved with the development of analytical methods such as gas chromatography (GC), thin-layer chromatography (TLC), and liquid chromatography (LC). The conventional GC and TLC methods require pre- or post-column derivation for detection [18–20]. The development of sophisticated MS has played a critical role in identifying and characterizing lipids from various biological samples over the last few decades. ESI–MS with tandem MS has dramatically affected omics studies analyzing the structure of complicated but biologically active molecules. While ESI–MS/MS provides a rapid analysis of lipids through a direct infusion, LC [21,22] before MS expands the ability to separate complicated lipid mixtures with minimal ionization suppression during MS analysis. In addition, comprehensive structural determination of lipid molecules by data-dependent MS/MS analysis [14,23–25] and the use of a capillary column at nanoflow rate scale for LC-ESI-MS/MS offers increased sensitivity with a ~1 fmol limit of detection from plasma samples [26].

In this study, relative abundance of lipids from plasma and urine samples from patients with GD were profiled both qualitatively and quantitatively with nanoflow LC–ESI–MS/MS. This work focused on distinguishing PLs, especially SLs (in particular MHC, DHC, and SM), from patients with GD that differed significantly from healthy controls. The change in targeted lipid levels in plasma and urine samples both from same GD patients was examined before and after each ERT treatment.

2. Experimental

2.1. Materials and reagents

Fourteen PL standards (16:0-lysophosphatidylcholine (LPC), 18:0-lyso phosphatidylethanolamine (LPE), 18:0/18:0-PC, 18:0/18:0-PE, 18:0-lysophosphatidic acid (LPA), 18:0-lysophosphatidylglycerol (LPG), 18:0-lysophosphatidylserine (LPS), 16:0/16:0-PA, 18:0/18:0-PG, 15:0/15:0-PG, 16:0/18:1-phosphatidylinositol (PI), 16:0/16:0-PS, d18:1/12:0-SM, and $(18:1)_4$-cardiolipin (CL) were purchased from Avanti Polar Lipids, Inc. (Alabaster, AL, USA), and six Cer standards (d18:1/16:0-GalCer, d18:1/18:0-GluCer, d18:1/16:0-LacCer, d18:1/14:0-Cer, d18:1/22:0-Cer, and d18:1/24:0-THC) were from Matreya, LLC (Pleasant Gap, PA, USA). 15:0/15:0-PG was directly added to urine and plasma samples as an internal standard (IS). All lipid standards were diluted to 30 pmol/μL in CH_3OH:CH_3CN (9:1, v/v). The mixture was stored at 4 °C until use. All organic solvents for lipid extraction including CH_3OH, $CHCl_3$, and methyl-*tert*-butyl ether (MTBE) were purchased from Sigma–Aldrich (St. Louis, MO, USA). All solvents for the LC mobile phase (CH_3CN, isopropanol, and CH_3OH) were of HPLC grade and purchased from Avantor Performance Materials (Center Valley, PA, USA). NH_4HCO_2 and NH_4OH for ionization modifiers were purchased from Sigma–Aldrich.

Plasma and urine samples from 15 healthy controls and 3 patients with GD were collected under informed consent from Severance Hospital (Seoul, Korea) at Yonsei University on the day of the clinical intervention before and 2 h after treatment and this study was approved by Institutional Review Board. All patients with GD in this study were diagnosed with type I disease.

2.2. Evaluation of lipid extraction methods

Because the efficiency of simultaneously extracting different categories of lipids, such as PLs and SLs, varies among methods, 3 methods (Bligh and Dyer [27], Folch with $CHCl_3$ [28], and the modified Folch with MTBE/CH_3OH [29]) were tested using lipid standards added to human urine. Fifteen microliters of 30-pmol/μL lipid standard mixture was added to 985 μL of urine from a healthy control and dried by vacuum centrifugation overnight.

2.2.1. Bligh and Dyer

The dried lipids from the urine sample spiked with standard lipids were dissolved in 300 μL of CH_3OH and 250 μL of $CHCl_3$. After vortexing for an hour, 250 μL of $CHCl_3$ and 450 μL of MS-grade H_2O were added, followed by vortexing for 10 min. The solution was then centrifuged at 1000 × *g* for 10 min, resulting in a distinct separation between the organic and aqueous layers. The lower organic layer was carefully pipetted into a pre-weighed Eppendorf tube, dried under vacuum centrifugation, dissolved in $CHCl_3$:CH_3OH (1:1, v/v), and diluted to 2 pmol/μL in CH_3OH:CH_3CN (9:1, v/v) for nLC–ESI–MS/MS.

2.2.2. Folch with $CHCl_3$

The dried lipid mixture was dissolved in 300 μL of CH_3OH and vortexed briefly before adding 600 μL of $CHCl_3$. After an hour of vortexing, 180 μL of MS-grade H_2O was added to the mixture and vortexed again for 10 min. The rest of the extraction steps were the same as the Bligh and Dyer method.

2.2.3. Modified Folch with MTBE/CH_3OH

The dried lipid mixture was dissolved in 300 μL of CH_3OH and vortexed briefly before adding 1000 μL of MTBE. After an hour of vortexing, 250 μL of MS-grade H_2O was added and vortexed for 10 min to induce phase separation. After centrifuging for 10 min at 1000 × *g*, the upper organic layer was pipetted to a new tube. Three hundred microliters of CH_3OH was added to the lower layer and sonicated for 2 min. After centrifuging at 1000 × *g* for 10 min, the upper organic layer was again collected and combined with the previously collected organic layer. This mixture was dried under vacuum centrifuge overnight. The final dried powder was diluted for nLC-ESI-MS/MS analysis as described in Section 2.2.1.

2.3. Lipid extraction from human plasma and urine samples

Lipids were extracted from 50-μL aliquot of plasma and 2000 μL of urine (15 controls and 3 patients with GD) according to the modified Folch with MTBE/CH_3OH procedure. At the final de-solvation step, weights of dried plasma and urinary lipids of each sample were measured, dissolved, and diluted to 20 μg/μL for plasma and 30 μg/μL for urine by using CH_3OH:CH_3CN (9:1, v/v) as a dispersing solvent. The reason for leveling each individual sample extract to the same concentration rather than dissolving all samples in the same volume of CH_3OH:CH_3CN was to avoid any possibility of low abundant lipid species from not being detected by MS because they

were below limit of detection (this often happens when amount of lipids present in individual sample varies, especially for urine). For the adjustment of total lipid concentration, the peak area of each species was multiplied by volume factor (volume of CH_3OH:CH_3CN added).

2.4. Lipid profiling by nLC–ESI–MS/MS

An LTQ Velos ion trap mass spectrometer from Thermo Finnigan (San Jose, CA, USA) with a model 1200 capillary pump system including an autosampler from Agilent Technologies (Palo Alto, CA, USA) was used to analyze lipids from plasma and urinary lipids. An analytical column made from a silica capillary tube (75 μm I.D. with 360 μm O.D.) was prepared in the laboratory. One end of the capillary column was pulled with a flame to make a sharp needle for a direct emitter to ESI. The column was packed with C18 resin beads, Watcher ODS-P (3 μm and 100 Å) purchased from Isu Industry Corp. (Seoul, Korea), under He (1000 psi) to a column length of 6 cm. The analytical column was connected to the capillary tubing from the LC pump with a PEEK microcross from IDEX (Oak Harbor, WA, USA). The other 2 ports of the microcross were connected to a Pt wire for the ESI voltage source and a vent capillary (20 μm I.D.) for split flow. The end of the vent capillary was attached to the on/off switch valve for the split and injection modes. nLC separation was carried out with gradient elution using 2 mobile phases: H_2O:CH_3CN (9:1, v/v) with 5 mM NH_4HCO_2 and 0.05% NH_4OH as modifiers for mobile phase A and CH_3OH:CH_3CN:isopropanol (2:2:6, v/v/v) with the same modifiers for phase B.

Samples were loaded onto the analytical column with mobile phase A at a 600 nL/min flow rate for 10 min with the switch valve off. After loading, gradient elution began by ramping mobile phase B from 0% to 80% over 10 min, then to 100% over next 20 min. Phase B was maintained at 100% for another 20 min for additional elution and washing. During the gradient elution, the pump delivered 10 μL/min to minimize dwell time, and the column flow rate was kept at 300 nL/min by using a vent capillary with the switch valve on. For nLC–ESI–MS/MS analysis, 15:0/15:0-PG was mixed with each sample as an internal standard (IS) after the extraction and for each run, 40 μg of extracted plasma lipids and 80 μg of extracted urinary lipids were injected. For each injection, 500 fmol of 15:0/15:0-PG was used as an internal standard (IS). Each sample was examined in triplicate and the home-made analytical column was utilized for the 150 consecutive injections of lipid extracts (4 μL each injection) from plasma or urine samples. For MS analysis, 3.0 kV was applied for ESI in negative ion mode with a mass range of 350–1200 amu for the precursor run followed by data-dependent collision induced dissociation (CID) analysis at 40% of normalized collision energy. The isolation width was set at m/z 2.0 with the neutral loss of m/z 60 (from $[M+HCO_2]^-$ to $[M-CH_3]^-$) for LPC, PC, and SM and of m/z 46 (from $[M+HCO_2]^-$ to $[M-H]^-$) for Cer, MHC, DHC, and THC. The structural determination of LPC, PC, and SM species was based on the fragment ion spectra from MS^3 while all other lipid species were identified by MS^2. Lipid molecular structures were identified with LiPilot, a computer algorithm developed in our laboratory [30]. To quantify lipid species in control and patient samples during drug intervention, the peak area of each precursor ion peak, which was pre-determined from nLC–ESI–MS^n analysis, was compared.

3. Results and discussion

Fig. 1a presents nLC–ESI–MS separation of 16 lipid standards (a). The same run conditions were used to separate lipid extracts from plasma and urine samples from patients with GD in Fig. 1b and c, respectively. The nLC run in Fig. 1 was performed by adding the mixed modifier [31] (0.05% NH_4OH and 5 mM NH_4HCO_2) in both mobile phases so that PLs of all classes (neutral polar PLs, such as PC and SM in the form of formate adducts, $[M+HCO_2]^-$, and most anionic lipids in the form of $[M-H]^-$) together with Cer and CL could be detected in negative ion mode. When analyzing different categories of lipids, such as PLs and SLs, simultaneously from patient samples, the lipid extraction method must be examined since different methods extract different lipids with varying efficiencies. Table 1 summarizes the average percent recoveries of lipid standards added to human urine from 3 different lipid extraction methods, Bligh and Dyer, Folch with $CHCl_3$, and modified Folch with MTBE/CH_3OH, over three consecutive runs. The extracted lipids were mixed with the IS right before being introduced to nLC–ESI–MS/MS, and its final concentration was 1 pmol/μL for extracted lipids. As 2 μL of sample was injected for each run, Table 1 reflects average recoveries of lipids at 2 pmol level. For the 18 lipid standards, the modified Folch with MTBE/CH_3OH outperformed the other methods for 15 species and had slightly lower efficiency for the other three species (LPE, PE, and CL). With the modified Folch with MTBE/CH_3OH method, 13 species were recovered at higher than 90% efficiency, and five species had yields between 82% and 90%. These recovery efficiencies can be considered reasonable. The other two methods had recoveries as low as 62–72%. The overall recovery of PL and SL standards spiked in a urine sample was higher for the modified Folch with MTBE/CH_3OH method than for the other two methods, which is similar to the results previously obtained for plasma sample [29]. PLs and SLs were simultaneously

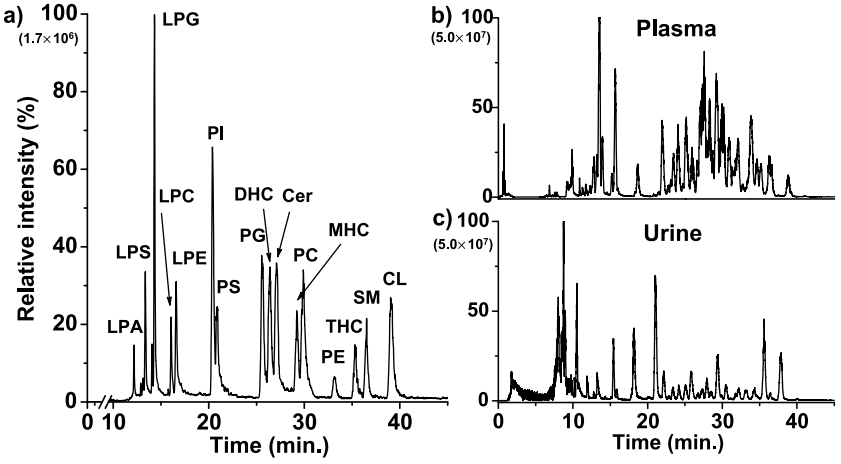

Fig. 1. Separation of (a) lipid standards, (b) plasma lipids, and (c) urinary lipids by nLC–ESI–MS/MS in negative ion mode.

Table 1
Average percent recoveries of 18 PL and SL standards added to human urine with three lipid extraction methods from 3 runs for each.

Class	Molecular species	*m/z*	Bligh and Dyer	Folch with $CHCl_3$	Modified Folch with MTBE/CH_3OH
LPC	16:0	540.4	86 ± 5	88 ± 6	92 ± 7
PC	16:0/16:0	778.5	91 ± 6	96 ± 5	98 ± 6
LPE	18:0	480.4	66 ± 5	89 ± 8	88 ± 6
PE	18:0/18:0	746.5	79 ± 3	90 ± 3	85 ± 5
LPA	18:0	437.5	77 ± 7	73 ± 5	91 ± 5
PA	16:0/16:0	647.5	78 ± 7	75 ± 5	91 ± 6
LPG	18:0	511.4	66 ± 4	90 ± 6	96 ± 5
PG	18:0/18:0	777.4	94 ± 5	96 ± 6	99 ± 6
PI	16:0/18:2	833.4	81 ± 6	90 ± 5	92 ± 5
LPS	18:0	524.4	63 ± 6	82 ± 5	95 ± 6
PS	16:0/16:0	734.4	85 ± 5	86 ± 4	89 ± 5
CL	$(18:1)_4$	727.8	81 ± 5	86 ± 5	82 ± 4
SM	d18:1/12:0	691.4	94 ± 5	98 ± 5	99 ± 3
Cer	d18:1/14:0	554.6	86 ± 5	82 ± 5	94 ± 5
	d18:1/22:0	666.6	88 ± 4	86 ± 5	90 ± 6
MHC	d18:1/18:0	772.6	83 ± 5	87 ± 4	98 ± 4
DHC	d18:1/16:0	906.6	85 ± 4	88 ± 5	98 ± 3
THC	d18:1/24:0	1180.6	81 ± 4	84 ± 4	94 ± 5

extracted from human plasma and urine by the modified Folch with MTBE/CH_3OH method in this study.

The extracted lipid mixtures from control and patient samples were analyzed by nLC–ESI–MS^n in negative ion mode. Molecular structures were determined from the characteristic CID fragment spectra. Fig. 2 shows examples of how molecular structures of glycosylated Cer (d18:1/16:0-MHC and d18:1/16:0-DHC) from human plasma sample were identified by MS/MS/MS (MS^3). The upper left spectrum of Fig. 2a shows the precursor scan of Fig. 1b at t_r = 26.42 min. A CID spectrum of a precursor ion with an *m/z* of 744.60 ($[M+HCO_2]^-$) yielded a product ion with an *m/z* of 698.49 ($[M-H]^-$) in the first CID experiment (MS^2). This change resulted from the loss of a formate and proton, and the MS^3 spectra of $[M-H]^-$ showed characteristic fragment ions. The secondary CID experiments of the $[M-H]^-$ ion of *m/z* 698.49 showed an intense peak at *m/z* 536.40. This peak was characterized by the loss of hexose ($[M-H-Hex]^-$) along with peaks resulting from the loss of H_2O and CH_2O from ($[M-H-Hex]^-$) and the dissociation of the acyl chain, which resulted in a free carboxylic anion detected at *m/z* 255.2 ($[RCOO]^-$). These results indicated that *m/z* 744.60 was the formate adduct form ($[M+HCO_2]^-$) of d18:1/16:0-MHC. A similar pattern of fragmented ions is shown in Fig. 2b for d18:1/16:0-DHC (t_r = 25.54 min of Fig. 1b), except that DHC consists of two hexose groups. Therefore, additional ions resulting from the cleavage of 2 hexose groups ($[M-H-2Hex]^-$ at *m/z* 536.44) were observed along with those from the cleavage of a single hexose $[M-H-Hex]^-$. More diverse lipid species were identified from plasma than from urine: 125 species from plasma and 105 from urine, as listed in Table S1 of Supporting Information. Many more LPC, PC, LPE, LPA, and Cer species were discovered from plasma. Approximately an equal number of PE, LPG, PA, PG, SM, MHC, and DHC species were identified in both plasma and urine. LPI, LPS, PS, and CL were detected in urine only, emphasizing the significance of analyzing urinary lipids although plasma is richer in lipids than urine. The observed trends from plasma samples were similar to those reported in literature [32,33].

To quantify the identified lipids, the concentration of each lipid species was determined from the average peak area of corresponding species, obtained from 3 nLC–ESI–MS/MS runs per sample. Because a constant concentration of internal standard,

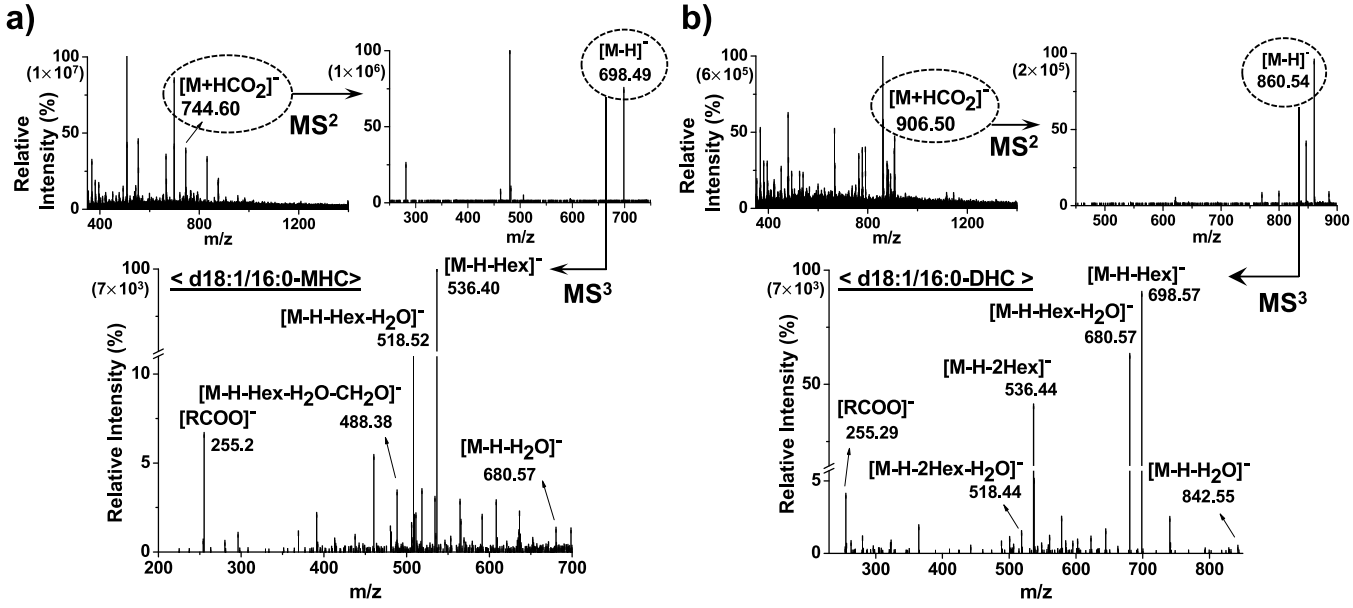

Fig. 2. (a) Parent ion MS scan (upper left) from plasma lipids at t_r = 26.42 min, MS^2 spectrum of the parent ion *m/z* 744.6 (d18:1/16:0-MHC), and MS^3 spectrum of *m/z* 698.5. (b) Parent ion MS scan from plasma lipids at t_r = 25.54, MS^2 spectrum of the parent ion *m/z* 906.5 (d18:1/16:0-DHC), and MS^3 spectrum of *m/z* 860.5.

Table 2
PL and SL species from plasma and urine with greater than 2-fold changes in concentration (marked in bold) between controls (n = 15 for plasma and urine) and patients with Gaucher disease ($n_{\text{plasma before therapy}}$ = 3, $n_{\text{plasma after therapy}}$ = 3, $n_{\text{urine before therapy}}$ = 3, $n_{\text{urine after therapy}}$ = 2).

Class	Molecular species	m/z	Plasma		Urine	
			Before therapy/controls	After therapy/controls	Before therapy/controls	After therapy/controls
PC	16:0/16:1	776.6	**2.27 ± 0.92**	**2.08 ± 0.76**	N.D.	N.D.
	16:1/20:4	824.5	**3.44 ± 1.75**	**2.64 ± 1.23**	N.D.	N.D.
	16:0/20:5	824.6	**2.44 ± 1.63**	**2.05 ± 1.13**	1.76 ± 0.78	1.22 ± 0.47
	16:0/22:6	850.6	**2.76 ± 1.37**	**1.53 ± 0.77**	1.93 ± 0.75	1.61 ± 0.56
	16:0/18:1	804.6	1.73 ± 0.67	1.48 ± 0.60	**2.08 ± 0.87**	**1.32 ± 0.53**
	16:0/22:5	852.6	**2.63 ± 1.15**	**1.78 ± 0.78**	**2.02 ± 0.79**	**1.05 ± 0.45**
	18:0/20:5	852.6	**2.43 ± 1.01**	**1.79 ± 0.62**	N.D.	N.D.
	18:0/22:6	878.6	**3.91 ± 1.83**	**2.69 ± 1.15**	1.31 ± 0.55	1.01 ± 0.40
	18:0/22:5	880.6	**2.40 ± 0.99**	**1.61 ± 0.80**	N.D.	N.D.
	18:0/18:1	832.5	1.78 ± 0.59	1.66 ± 0.80	**3.36 ± 1.38**	**1.22 ± 0.47**
LPE	22:6	524.3	**2.98 ± 1.66**	**2.83 ± 1.15**	N.D.	N.D.
PE	16:0/18:1	716.6	**3.10 ± 1.40**	**2.61 ± 1.17**	1.43 ± 0.66	0.83 ± 0.36
PI	16:0/16:1	807.4	**3.19 ± 1.54**	**2.96 ± 1.32**	N.D.	N.D.
	16:0/16:0	809.6	1.42 ± 0.83	1.42 ± 0.22	**2.15 ± 0.86**	**2.51 ± 1.25**
	16:0/18:2	833.6	**2.99 ± 1.13**	**2.98 ± 1.17**	1.35 ± 0.62	0.99 ± 0.41
	16:0/20:4	857.6	**3.31 ± 1.33**	**3.98 ± 1.79**	1.23 ± 0.57	0.73 ± 0.36
	16:0/22:6	881.6	**2.61 ± 1.53**	**3.28 ± 1.62**	1.27 ± 1.00	0.94 ± 0.48
Cer	d18:1/16:0	581.7	**2.46 ± 1.18**	**1.84 ± 0.92**	1.35 ± 0.51	1.15 ± 0.41
	d18:1/18:0	609.7	**2.54 ± 1.33**	**2.06 ± 1.11**	N.D.	N.D.
	d18:1/24:0	694.8	1.03 ± 0.45	1.27 ± 0.58	**2.48 ± 1.55**	**1.35 ± 0.75**
MHC	d18:1/16:0	744.7	**2.98 ± 1.35**	**2.43 ± 0.89**	**2.38 ± 0.91**	**1.26 ± 0.49**
	d18:1/20:0	800.6	N.D.	N.D.	**3.04 ± 1.13**	**2.59 ± 1.11**
	d18:1/22:0	828.7	**3.53 ± 0.73**	**2.38 ± 0.59**	**3.19 ± 1.53**	**1.25 ± 0.41**
	d18:1/24:1	854.7	**3.85 ± 1.63**	**2.96 ± 1.11**	**3.42 ± 1.77**	**1.40 ± 0.33**
	d18:1/24:0	856.7	**3.84 ± 1.53**	**2.84 ± 1.13**	1.91 ± 0.73	1.30 ± 0.50
DHC	d18:1/24:0	1018.6	0.90 ± 0.47	0.99 ± 0.46	**3.46 ± 1.85**	**1.54 ± 0.62**

15:0/15:0-PG, was injected with each sample to compensate for fluctuations in MS intensity across different runs, the peak area of each lipid species was normalized to the internal standard (500 fmol per each injection). The peak area of each individual component was multiplied by a volume factor, which was the volume of solvent added to disperse the lipid extract, to adjust the total lipid concentration.

Although plasma and urine samples were collected from the same individuals, the plasma lipid profile was different from the urine profile. Some species were detected in either plasma or urine exclusively, such as d18:1/20:0-MHC, which was detected in urine only, and d18:1/14:0-SM, which was detected in plasma only. Although many species were identified from both sources, they were identified at different concentrations. For example, the concentration of urinary 16:0-LPA was relatively high comparing with other urinary lipids as the peak area ratios of many species were below 1 (relative to 500 fmol of IS) but opposite trend was observed in plasma; comparing to other plasma lipids such as PC species whose overall peak area ratios were well over 1, the relative peak area of plasma 16:0-LPA was only 0.3–0.36, hinting that its concentration is relatively low in urine, as shown in Table S1.

Table 2 summarizes the list of selected lipid species, showing greater than 2-fold differences between controls and patients using the Mann–Whitney U-test and p-values < 0.02. The values are ratios of average peak areas and standard deviations of lipid species from patients before and after therapy compared with those from controls. Of 125 plasma and 105 urinary lipids, 20 plasma species (8 PC, 1 LPE, 1 PE, 4 PI, 2 Cer, and 4 MHC) and 10 urinary species (3 PC, 1 PI, 1 Cer, 4 MHC, and 1 DHC), all marked in bold, differed significantly between controls and patients. The points plotted in Fig. 3 represent the peak areas of all urinary species listed in Table 2, from controls (n = 15, filled triangles), patients before therapy (n = 3, open circles), and patients after therapy (n = 2, filled circles) and plasma species are plotted in Fig. S1 of Supporting Information. In Fig. 3, clusters in individual groups of samples demonstrate distinct differences between controls and patients before therapy, especially all of the MHC species except d18:1/24:1-MHC. Low peak area ratios of MHC species indicate that they are

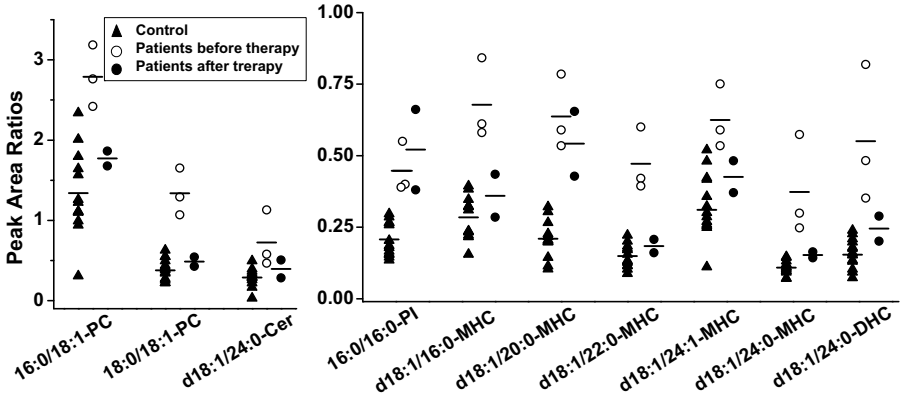

Fig. 3. Urinary PLs with a greater than a 2-fold difference between patients and controls and changes after ERT.

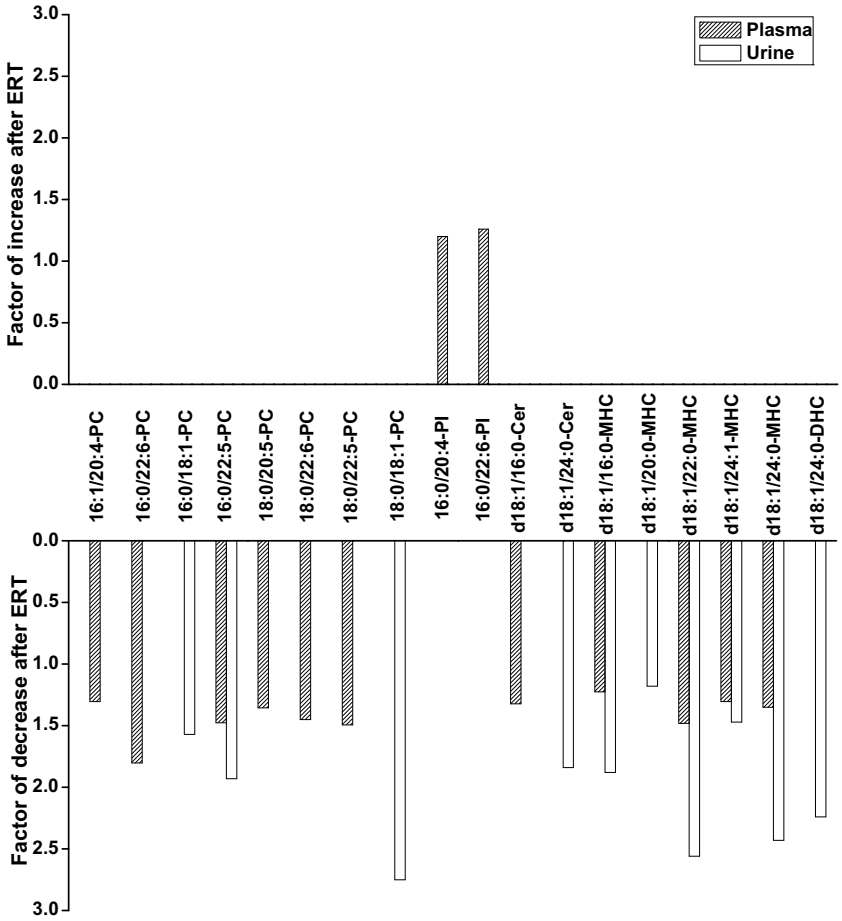

Fig. 4. Changes in relative concentration of selected PLs and Cers from plasma and urine samples plotted by the change after ERT.

low-abundance species unlike other species such as 16:0/18:1-PC on the left panel but more intense differences between patients and controls can be observed in these low-abundance MHC species. Also, compared to plasma species shown in Fig. S1, urinary species in Fig. 3 clearly display definite differences between controls and patients, rarely overlapping the similar levels of concentrations. For the average concentrations of the species before and after the therapy, all species except 16:0/16:0-PI decreased after therapy in unison and most of them were reduced down to concentrations of healthy controls, approximately. While a relatively large number of plasma PC species (8 of 26 PCs identified) are listed in Table 2, all 4 MHC species identified from plasma differed significantly, as reported in literature [3]. The concentrations of all plasma MHC species were roughly 3-fold higher in patients than in controls, and all decreased noticeably after ERT. All urinary species except d18:1/24:0-MHC had more than 2-fold increases in patients compared with controls. The d18:1/24:0-MHC concentration in patients was 1.91 times higher than that in controls, and it decreased by 2-fold after ERT. These results indicate that d18:1/24:0-MHC was affected by GD and ERT though to lesser degree than other MHC species. The concentrations of all urinary MHC species decreased by close to or greater than 2-fold after ERT, while plasma species decreased by lesser degree around 1.5-fold, as seen in Fig. 4. This result suggests that ERT affected urinary lipids more than it affected plasma lipids. This result could be due, in part, to chitotriosidase activity [34]. Chitotriosidase activity was reported to be increased by at least 100-fold in patients with GD comparing with healthy controls. Chitotriosidase activity can be controlled and corrected by ERT, but its activity was found to decrease more rapidly and significantly in urine than in plasma [35]. Because chitotriosidase activity was more affected in urine, urinary lipid levels could decrease to a greater degree than plasma lipids. The fact that the concentrations of all plasma and urinary MHC species decreased after ERT reflects the fact that ERT specifically targets MHC degradation. Unlike other lipid classes, where the change in concentrations after therapy differed, most PC species noticeably decreased after therapy. This observation can be partially explained by the relationship between MHC accumulation and PC synthesis. One study reported that MHC accumulation promoted PC synthesis in neurons [6], and a similar result might have been observed in plasma. Plasma and urinary d18:1/22:0-MHC and d18:1/24:1-MHC, urinary d18:1/16:0-MHC and d18:1/20:0-MHC, and plasma d18:1/24:0-MHC form discrete clusters of concentrations within a group of samples between controls and patients. The overall concentrations of plasma d18:1/16:0-MHC and urinary d18:1/24:0-MHC, however, did not differ much between patients and controls as other MHC species did. Therefore, the 2 latter species would be less significant for GD than other MHC species: d18:1/22:0-MHC, d18:1/24:1-MHC, and d18:1/24:0-MHC from plasma and d18:1/16:0-MHC, d18:1/20:0-MHC, d18:1/22:0-MHC, and d18:1/24:1-MHC from urine. Among the PC species, plasma 18:0/22:6-PC and 16:1/20:4-PC, and urinary 18:0/18:1-PC would be more significant than other PCs because they had greater than 3-fold differences.

4. Conclusion

This study validates the nLC–ESI–MS/MS method to identify characteristic lipid species that show significant differences

between healthy controls and GD patients based on relative quantification of lipids. A variety of lipids were observed in plasma and urine from both healthy controls and patients with GD by employing nLC–ESI–MS/MS which offered advantages including low limit of detection (0.3–9 fmol for various types of lipids [31]), reduced consumption of organic solvents, and increased ionization efficiency during ESI without splitting flow. Unlike other lipids, many PC species and all MHC species tended to decrease in patients after receiving ERT, indicating that ERT targeted these species. As seen in Table S1 of Supporting Information, the overall concentrations of MHC and DHC were rather small, especially in plasma, meaning that they are low-abundance species in humans. Even though their concentrations were lower than the concentrations of other lipid species, such as PL, the differences between controls and patients were definite (more than 2- or 3-fold changes). All MHC species were increased significantly higher among patients before ERT than controls and decreased after ERT. Therefore, these low-abundance MHC and DHC species are just as characteristic species as high-abundance PC species. As all MHC species increased significantly in both plasma and urine from patients, this study confirmed that MHC species were directly affected by dysfunctional lysosomes in GD, and all MHC concentrations decreased after ERT. The concentrations of urinary MHC decreased more rapidly than plasma species, partially supported by the fact that activity of chitotriosidase was affected by more in urine than plasma [33]. From this study, 20 plasma and 10 urinary lipids were selected as significant species of GD. Among these species, d18:1/16:0-, d18:1/22:0-, and d18:1/24:1-MHC differed significantly in both plasma and urine. d18:1/20:0-MHC and d18:1/24:0-MHC differed in urine only and plasma only, respectively. Overall, MHC species would serve as excellent candidates in developing an early diagnostic test for GD using both plasma and urine. Other PL and SL species should be considered in the future.

Acknowledgements

This study was supported by a grant (HI12C-0022-030014) of the Korea Healthcare technology R&D Project, Ministry of Health & Welfare and in part by a grant NRF-2010-0014046.

Appendix A. Supplementary data

Supplementary data associated with this article can be found, in the online version, at http://dx.doi.org/10.1016/j.chroma.2015.01.004.

References

[1] N.W. Barton, R.O. Brady, J.M. Dambrosia, A.M. Di Bisceglie, S.H. Doppelt, S.C. Hill, H.J. Mankin, G.J. Murray, R.I. Parker, C.E. Argoff, R.P. Grewal, K.-T. Yu, Replacement therapy for inherited enzyme deficiency-macrophage-targeted glucocerebrosidase for Gaucher's disease, N. Engl. J. Med. 324 (1991) 1464–1470.
[2] K. Wong, E. Sidransky, A. Verma, T. Mixon, G.D. Sandberg, L.K. Wakefield, A. Morrison, A. Lwin, C. Colegial, J.M. Allman, R. Schiffmann, Neuropathology provides clues to the pathophysiology of Gaucher disease, Mol. Genet. Met. 82 (2004) 192–207.
[3] P.J. Meikle, P.D. Whitfield, T. Rozaklis, D. Blacklock, S. Duplock, D. Elstein, A. Zimran, E. Mengel, P. Cannell, J.J. Hopwood, M. Fuller, Plasma lipids are altered in Gaucher disease: biochemical markers to evaluate therapeutic intervention, Blood Cell Mol. Dis. 40 (2008) 420–427.
[4] T.A. Burrow, S. Barnes, G.A. Grabowski, Prevalence and management of Gaucher disease, Pediatr. Health Med. Therapeut. 2 (2011) 59–73.
[5] J.M. Aerts, W.W. Kallemeijn, W. Wegdam, M. Joao Ferraz, M.J. van Breemen, N. Dekker, G. Kramer, B.J. Poorthuis, J.E. Groener, J. Cox-Brinkman, S.M. Rombach, C.E. Hollak, G.E. Linthorst, M.D. Witte, H. Gold, G.A. van der Marel, H.S. Overkleeft, R.G. Boot, Biomarkers in the diagnosis of lysosomal storage disorders: proteins, lipids, and inhibitors, J. Inherit. Metab. Dis. 34 (2011) 605–619.
[6] J. Bodennec, D. Pelled, C. Riebeling, S. Trajkovic, A.H. Futerman, Phosphatidylcholine synthesis is elevated in neuronal models of Gaucher disease due to direct activation of CTP:phosphocholine cytidylyltransferase by glucosylceramide, FASEB J. 16 (2002) 1814–1816.
[7] J.F. Brouwers, E.A. Vernooij, A.G. Tielens, L.M. van Golde, Rapid separation and identification of phosphatidylethanolamine molecular species, J. Lipid Res. 40 (1999) 164–169.
[8] M.M. Wright, A.G. Howe, V. Zaremberg, Cell membranes and apoptosis: role of cardiolipin, phosphatidylcholine, and anticancer lipid analogues, Biochem. Cell Biol. 82 (2004) 18–26.
[9] R. Meshkani, K. Adeli, Hepatic insulin resistance, metabolic syndrome and cardiovascular disease, Clin. Biochem. 42 (2009) 1331–1346.
[10] L. Slama, C. Le Camus, L. Serfaty, G. Pialoux, J. Capeau, S. Gharakhanian, Metabolic disorders and chronic viral disease: the case of HIV and HCV, Diabetes Metab. 35 (2009) 1–11.
[11] H.K. Min, S. Lim, B.C. Chung, M.H. Moon, Shotgun lipidomics for candidate biomarkers of urinary phospholipids in prostate cancer, Anal. Bioanal. Chem. 399 (2011) 823–830.
[12] S. Lim, D.Y. Bang, K.H. Rha, M.H. Moon, Rapid screening of phospholipid biomarker candidates from prostate cancer urine samples by multiple reaction monitoring of UPLC-ESI-MS/MS and statistical approaches, Bull. Kor. Chem. Soc. 35 (2014) 1133–1138.
[13] H. Kim, H.K. Min, G. Kong, M.H. Moon, Quantitative analysis of phosphatidylcholines and phosphatidylethanolamines in urine of patients with breast cancer by nanoflow liquid chromatography/tandem mass spectrometry, Anal. Bioanal. Chem. 393 (2009) 1649–1656.
[14] H.K. Min, G. Kong, M.H. Moon, Quantitative analysis of urinary phospholipids with breast cancer by nanoflow liquid chromatography-tandem mass spectrometry: II. Negative ion mode analysis of four phospholipid classes, Anal. Bioanal. Chem. 396 (2010) 1273–1280.
[15] R. Sutphen, Y. Xu, G.D. Wilbanks, J. Fiorica, E.C. Grendys Jr., J.P. LaPolla, H. Arango, M.S. Hoffman, M. Martino, K. Wakeley, D. Griffin, R.W. Blanco, A.B. Cantor, Y.J. Xiao, J.P. Krischer, Lysophospholipids are potential biomarkers of ovarian cancer, Cancer Epidemiol. Biomark. Prev. 13 (2004) 1185–1191.
[16] Z. Zhao, Y. Xiao, P. Elson, H. Tan, S.J. Plummer, M. Berk, P.P. Aung, I.C. Lavery, J.P. Achkar, L. Li, G. Casey, Y. Xu, Plasma lysophosphatidylcholine levels: potential biomarkers for colorectal cancer, J. Clin. Oncol. 25 (2007) 2696–2701.
[17] S.K. Byeon, J.Y. Lee, S. Lim, D. Choi, M.H. Moon, Discovery of candidate phospholipid biomarkers in human lipoproteins with coronary artery disease by flow field-flow fractionation and nanoflow liquid chromatography-tandem mass spectrometry, J. Chromatogr. A 1270 (2012) 246–253.
[18] H.Y. Kim, T.C.L. Wang, Y.C. Ma, Liquid chromatography/mass spectrometry of phospholipids using electrospray ionization, Anal. Chem. 66 (1994) 3977–3982.
[19] X. Han, R.W. Gross, Structural determination of lysophospholipid regioisomers by electrospray ionization tandem mass spectroscopy, J. Am. Chem. Soc. 118 (1996) 451–457.
[20] F.F. Hsu, J. Turk, Electrospray ionization/tandem quadrupole mass spectrometric studies on phosphatidylcholines: the fragmentation processes, J. Am. Soc. Mass Spectrom. 14 (2003) 352–363.
[21] G. Isaac, D. Bylund, J.E. Månsson, K.E. Markides, J. Bergquist, Analysis of phosphatidylcholine and sphingomyelin molecular species from brain extracts using capillary liquid chromatography electrospray ionization mass spectrometry, J. Neurosci. Methods 128 (2003) 111–119.
[22] R. Taguchi, J. Hayakawa, Y. Takeuchi, M. Ishida, Two-dimensional analysis of phospholipids by capillary liquid chromatography/electrospray ionization mass spectrometry, J. Mass Spectrom. 35 (2000) 953–966.
[23] R. Taguchi, T. Houjou, H. Nakanishi, T. Yamazaki, M. Ishida, M. Imagawa, T. Shimizu, Focused lipidomics by tandem mass spectrometry, J. Chromatogr. B 823 (2005) 26–36.
[24] S. Yu, Q. Li, T.M. Badger, N. Fang, Quantitative analysis of polar lipids in the nanoliter level of rat serum by liquid chromatography/mass spectrometry/mass spectrometry, Exp. Biol. Med. 234 (2009) 157–163.
[25] J.Y. Lee, H.K. Min, D. Choi, M.H. Moon, Profiling of phospholipids in lipoproteins by multiplexed hollow fiber flow field-flow fractionation and nanoflow liquid chromatography-tandem mass spectrometry, J. Chromatogr. A 1217 (2010) 1660–1666.
[26] D.Y. Bang, M.H. Moon, On-line two-dimensional capillary strong anion exchange/reversed phase liquid chromatography-tandem mass spectrometry for comprehensive lipid analysis, J. Chromatogr. A. 1310 (2013) 82–90.
[27] E.G. Bligh, W.J. Dyer, A rapid method for total lipid extraction and purification, Can. J. Biochem. Physiol. 37 (1959) 911–917.
[28] J. Folch, M. Lees, G.H. Sloane Stanley, A simple method for the isolation and purification of total lipids from animal tissues, J. Biol. Chem. 226 (1957) 497–509.
[29] S.K. Byeon, J.Y. Lee, M.H. Moon, Optimized extraction of phospholipids and lysophospholipids for nanoflow liquid chromatography–electrospray ionization–tandem mass spectrometry, Analyst 137 (2012) 451–458.
[30] S. Lim, S.K. Byeon, J.Y. Lee, M.H. Moon, Computational approach to structural identification of phospholipids using raw mass spectra from nanoflow liquid chromatography–electrospray ionization–tandem mass spectrometry, J. Mass Spectrom. 47 (2012) 1004–1014.
[31] D.Y. Bang, S. Lim, M.H. Moon, Effect of ionization modifiers on the simultaneous analysis of all classes of phospholipids by nanoflow liquid chromatography/tandem mass spectrometry in negative ion mode, J. Chromatogr. A 1240 (2012) 69–76.

[32] M. Murph, T. Tanaka, J. Pang, E. Felix, S. Liu, R. Trost, A.K. Godwin, R. Newman, G. Mills, Liquid chromatography mass spectrometry for quantifying plasma lysophospholipids: potential biomarkers for cancer diagnosis, Methods Enzymol. 433 (2007) 1–24.
[33] D.Y. Bang, S.K. Byeon, M.H. Moon, Rapid and simple extraction of lipids from blood plasma and urine for liquid chromatography–tandem mass spectrometry, J. Chromatogr. A 1331 (2014) 19–26.
[34] C.E.M. Hollak, S. Van Weely, M.H.J. Van Oers, J.M.F.G. Aerts, Marked elevation of plasma chitotriosidase activity. A novel hallmark of Gaucher disease, J. Clin. Invest. 93 (1994) 1288–1292.
[35] R.G. Boot, M. Verhoek, M. Langeveld, G.H. Renkema, C.E.M. Hollak, J.J. Weening, W.E. Donker-Koopman, J.E. Groener, J.M.F.G. Aerts, CCL18. A urinary marker of Gaucher cell burden in Gaucher patients, J. Inherit. Metab. Dis 29 (2006) 564–571.